

# Establishment and validation of a torsade de pointes prediction model based on human iPSC-derived cardiomyocytes

DONGSHENG PAN<sup>1,2</sup>, BO LI<sup>1,2</sup> and SANLONG WANG<sup>2</sup>

<sup>1</sup>Graduate School of Peking Union Medical College, Chinese Academy of Medical Sciences and Peking Union Medical College, Beijing 100730; <sup>2</sup>National Center for Safety Evaluation of Drugs, National Institutes for Food and Drug Control, Beijing 100176, P.R. China

Received June 8, 2022; Accepted September 26, 2022

DOI: 10.3892/etm.2022.11760

**Abstract.** Drug-induced cardiotoxicity is one of the main causes of drug failure, which leads to subsequent withdrawal from pharmaceutical development. Therefore, identifying the potential toxic candidate in the early stages of drug development is important. Human induced pluripotent stem cell-derived cardiomyocytes (hiPSC-CMs) are a useful tool for assessing candidate compounds for arrhythmias. However, a suitable model using hiPSC-CMs to predict the risk of torsade de pointes (TdP) has not been fully established. The present study aimed to establish a predictive TdP model based on hiPSC-CMs. In the current study, 28 compounds recommended by the Comprehensive *in vitro* Proarrhythmia Assay (CiPA) were used as training set and models were established in different risk groups, high- and intermediate-risk versus low-risk groups. Subsequently, six endpoints of electrophysiological responses were used as potential model predictors. Accuracy, sensitivity and area under the curve (AUC) were used as evaluation indices of the models and seven compounds with known TdP risk were used to verify model differentiation and calibration. The results showed that among the seven models, the AUC of logistic regression and AdaBoost model was higher and had little difference in both training and test sets, which indicated that the discriminative ability and model stability was good and excellent, respectively. Therefore, these two models were taken as submodels, similar weight was configured and a new TdP risk prediction model was constructed using a soft voting strategy. The classification accuracy, sensitivity and AUC of the new model were 0.93, 0.95 and 0.92 on the training set, respectively and all 1.00 on the

test set, which indicated good discrimination ability on both training and test sets. The risk threshold was defined as 0.50 and the consistency between the predicted and observed results were 92.8 and 100% on the training and test sets, respectively. Overall, the present study established a risk prediction model for TdP based on hiPSC-CMs which could be an effective predictive tool for compound-induced arrhythmias.

## Introduction

Drug-induced arrhythmias are new or exacerbated existing arrhythmias in patients during or after drug treatment and are the most common clinical adverse cardiovascular events (1). Drug-induced TdP is serious and fatal and multiple compounds were recalled in the 1990s and early 2000s due to TdP (2). As such, drug-related arrhythmia is one of the main causes of drug withdrawal and drug recalls and how to predict drug-induced TdP is a key problem in drug research and development (3).

Human ether-a-go-go related gene (hERG) block and QT prolongation are thought to be the main causes of TdP (4). Consequently, the International Council on Harmonization of Technical Requirements for Registration of Pharmaceuticals for Human Use issued guidelines S7B and E14 in 2005 (5). S7B recommends *in vitro* assays to evaluate whether compounds and their metabolites block hERG currents, while E14 focuses on the overall clinical QT monitoring to determine whether the drugs prolong QT (6). These two are currently the main guidelines for the safety evaluation of drug-induced arrhythmias.

The implementation of these two guidelines effectively reduces cardiotoxicity risk in the later drug development stage (7). However, hERG block and QT prolongation are sensitive but not specific to TdP risk identification (8). Cardiomyocyte repolarization is a complex process resulting in multiple time- and voltage-dependent ion flows across membrane (9). In addition, hERG is an important outward potassium current during repolarization and hERG block can lead to prolonged repolarization and prolonged QT interval (4). Nevertheless, it does not induce QT prolongation if a compound, for instance verapamil, blocks both outward potassium and inward calcium currents (10). Therefore, drug-induced hERG block cannot be definitively proven to be exclusively associated with QT prolongation or TdP (11).

---

*Correspondence to:* Professor Sanlong Wang, National Center for Safety Evaluation of Drugs, National Institutes for Food and Drug Control, A8 Hongda Middle Street, Beijing Economic-Technological Development Area, Beijing 100176, P.R. China  
E-mail: wangsanlong@nifdc.org.cn

**Key words:** drug-induced arrhythmias, human induced pluripotent stem cell derived-cardiomyocytes, torsade de pointes, prediction model, field potential

The Food and Drug Administration (FDA) launched the CiPA program in 2013 that proposed a new mechanism and model information approach to evaluate cardiac safety of new drugs (12). The initiative focuses on the effects of drugs on multiple ion channels using computer models to simultaneously grade the risk of arrhythmias along with a validation assessment using hiPSC-CMs and evaluates the expected risk of drugs in phase I of clinical study (13). A key CiPA principle is that ventricular repolarization and TdP depend on changes in the equilibrium of ion flows in and outside the cell membrane and is not solely on hERG blockade (14). Moreover, hiPSC-CMs are more suitable for the evaluation of arrhythmias compared with the noncardiac myocytes stably transfected with the human hERG gene. hiPSC-CMs express cardiocontractile proteins and functional ion channels, which ensure that the cells simulate the function of the human conduction system (15,16). Thus, it has become the preferred model to predict TdP (17).

Previous studies of TdP prediction models have mainly been based on the electrophysiological effects of compounds on hiPSC-CMs, commonly employing regression- and machine learning-based methods (18). Ando *et al.* (17) established a regression-based risk prediction model based on field potential duration (FPD) prolongation and early afterdepolarization, which has been used for risk score prediction of TdP risk. In addition, da Rocha *et al.* (19) established a regression-based TdP risk model based on the Voltage Sensitive Dye Assay and used only a single predictor, action potential (AP). Raphael *et al.* (20) constructed an algorithm based on the modelling dictionary and greedy optimization to predict the risk of proarrhythmia using hiPSC-CMs and used FPD prolongation as a model predictor. The prediction model published in the 2018 FDA report included seven predictors but only used one algorithm, LR model (21). Single predictor models are prone to false positive and false negative results in the application and a single algorithm, especially logical regression, which may not be able to identify some significant non-linear relations and detect the correlation between predictive variables, is prone to result in a false-negative practical application (22). Machine learning techniques overcome the shortcomings of traditional regression-based methods and have excellent performance in predictive models (23). In addition, machine learning can predict accurately using multiple predictors following nonlinear links and interaction between multiple variables (24).

In the present study, the effects of compounds on the electrophysiology of synergistically beating 2D cardiomyocytes on a label-free cardiac safety screening device were examined. A total of 28 CiPA compounds (eight high, 11 intermediate and nine low TdP risk) were used as training set. Overall, six endpoints of electrophysiological responses were used as model predictors and seven models were selected. Subsequently, two models [LR and Adaptive Boosting (AdaBoost)] with high accuracy and good stability were selected as sub-models, establishing a new TdP prediction model with higher accuracy and sensitivity. This model is predicted to reduce the impact of differences in species and reduce the evaluation shortcomings caused by the use of hERG inhibition as a single indicator. This model is expected to be used for preclinical drug-induced TdP prediction and also for the re-evaluation of post-marketing drugs.

## Materials and methods

**hiPSC-CMs culture.** hiPSC-CMs (cat. no. CA2201106; Beijing Cellapy Biotechnology Co., Ltd.) were cryopreserved in liquid nitrogen (approx.  $-196^{\circ}\text{C}$ ) for  $\sim 30$  days after differentiation. The cardiomyocytes used in the present study consist mainly of ventricular myocytes with autonomous electrophysiological activity, but also contain a small proportion of atrial myocytes and sinoatrial node-like cells. Cell culture was conducted following the manufacturer's protocols and four batches of hiPSC-CMs were used. Briefly,  $5\ \mu\text{l}$  fibronectin ( $50\ \mu\text{g}/\text{ml}$ , cat. no. F2006; Sigma-Aldrich; Merck KGaA) was added to the central electrode of the CardioExcyte 96 sensor plates (cat. no. 020730; Nanion Technologies GmbH), then the plate was incubated at  $37^{\circ}\text{C}$  for 1-1.5 h. The cells were then thawed in a  $37^{\circ}\text{C}$  water bath and centrifuged at  $200 \times g$  for 5 min at room temperature. The supernatant was later discarded and the cell concentration was adjusted to  $4\text{-}5 \times 10^4$  cells/ml. Fibronectin coating solution from the sensor plate was discarded and  $5\ \mu\text{l}$  of cell suspension was added into each well before being incubated for 1 h at  $37^{\circ}\text{C}$ , 5%  $\text{CO}_2$ . Lastly,  $200\ \mu\text{l}$  of medium (cat. no. CA2015002; Cellapy; Beijing Saibei Biotechnology Co., Ltd.) was added to each well and the plate was cultured for 14-21 days at  $37^{\circ}\text{C}$ , 5%  $\text{CO}_2$ . The medium was replaced 48 h after plating and medium changing was performed every other day.

**Test compounds.** In total, 35 compounds were used (17 were purchased from Sigma-Aldrich, Merck KGaA; 16 were made by medicinal chemists at the National Institute for Food and Drug Control; one from Selleck Chemicals; and one from MedChemExpress). All compounds were dissolved in DMSO or  $\text{H}_2\text{O}_2$  to prepare the stock solutions, which were at least 1,000 times more concentrated compared with the highest concentration used experimentally (Table S1).

**Myocardial cell activity, beat frequency and field potential detection.** The sensor plate was placed on the CardioExcyte 96 and incubated at  $37^{\circ}\text{C}$  for 1-2 days before drug administration. The medium was changed on the day of drug administration. Different compounds ( $100\ \mu\text{l}$ ) were added 3-4 h after culture medium change and 0.1% DMSO was set as the negative control for each plate. The data collection interval was 30 min within 2 h, the interval then changed to 2 h. Thus, the data collection period was  $>24$  h. For each experiment, three to four concentrations were set for each compound and three duplicates were set for each concentration. Each experiment was repeated in duplicate or quadruplicate. Data for nicotinamide and mannitol were from a single experiment and eight replicates were set for each concentration. The main indices were amplitude (Ampl), the representative amplitude traces were shown in Fig. S1, beats per minute (BPM) and FPD. FPD was corrected to FPDc by Fridericia's formula:

$$\text{FPDc} [\text{ms}] = \frac{\text{FPD} [\text{ms}]}{\sqrt[3]{\text{ISI} [\text{s}]}}$$

FPD, Field potential duration; ISI, Inter-spike interval.

**Recording of arrhythmia-like waveforms.** Asakura *et al.* (25) recorded the compound-induced arrhythmia waveforms; an arrhythmia-like waveform was observed and recorded as 1 and without arrhythmia-like waveforms was recorded as 0.

**Data processing.** CardioExcyTecontrol (version 1.4.5.6; Nanion Technologies GmbH) software was used to process the data. The negative control, 0.1% DMSO, was used as the baseline to calibrate the online analysis parameters. Ampl, BPM and FPDc (Corrected FPD) data were then normalized to preadministration data. The FPDc change was calculated according to the following formula:

$$\% \text{ Change in FPDc} = \frac{\text{FPDc after treatment}}{\text{FPDc before treatment}} \times 100$$

**Model establishment and evaluation.** In total, 28 CiPA compounds were used as the training set. In addition, a prediction model of TdP risk was constructed following the physiological effects of these compounds on hiPSC-CMs. effective therapeutic plasma concentration (ETPC), arrhythmia-like events, drug concentration (folds over ETPC when drug-induced arrhythmias were first observed), type of FPDc change, the degree of change in FPDc and drug concentration (folds over ETPC) at which the change of FPDc was observed (Table I) were used as model predictors. Based on these six predictors, seven models were established in the training set for high- and intermediate-risk compounds versus low-risk compounds. The seven models were LR, Support Vector Machine (SVM), *k*-nearest neighbor algorithm (KNN), decision tree (DT), AdaBoost, CatBoost and Random Forest (RF).

Accuracy, recall rate or sensitivity and AUC were used to evaluate the ability to distinguish capacity, where the larger the index value is, the higher the prediction ability of the model is (26,27). Seven compounds with known TdP risk were used as the test set to evaluate the calibration capacity-defined as the consistency between predicted and observed results (28). The models with excellent comprehensive performance and good stability in the training and test data sets were selected and the voting classifier strategy was then used for model training. Each sub-model was assigned a similar weight and the new voting classifier (VC) prediction model was established through soft voting; the weight here refers to the relative importance of the indicator in the overall evaluation. The VC model is the combination of two classifiers that combined the predicted probabilities for each classifier and the highest probability is then voted (Fig. 1).

**Statistical analysis.** Data are expressed as the mean  $\pm$  standard deviation. SPSS 26.0 (IBM Corp) was used to perform Pearson's and Spearman's correlation analysis,  $P < 0.05$  was considered to indicate a statistically significant difference. Python 3.8.0 (python.org/) and Prism 8.0 (GraphPad Software, Inc.) were used to establish prediction models and plot data.

## Results

**Effects of compounds on myocardial cell activity and beating frequency.** Ampl is an impedance parameter, which is a key parameter for the estimation of cell viability (29). In total, four out of eight high TdP risk compounds resulted in decreased cell viability (Fig. 2), among which, disopyramide, ibutilide and quinidine could cause decreased cell activity at concentrations less than ETPC. Moreover, nine (Astemizole, Chlorpromazine, Cisapride, Clarithromycin, Droperidol, Ondansetron, Pimozide, Risperidone and Terfenadine) out of eleven and eight (Diltiazem, Loratadine, Metoprolol, Mexiletine,

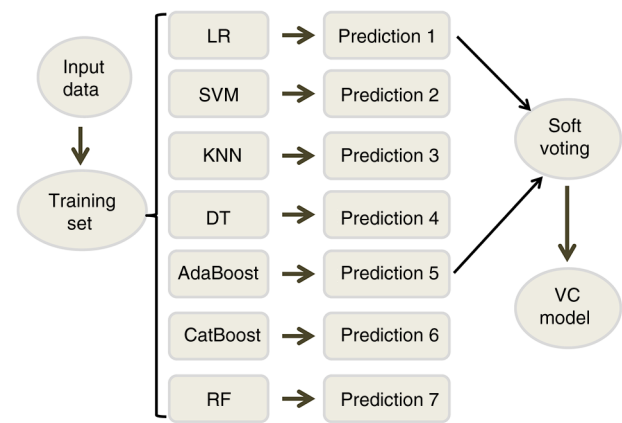


Figure 1. Flow chart depicting the prediction model with soft voting. LR, logistic regression; SVM, support vector machine; KNN, *k*-nearest neighbor algorithm; DT, decision tree; RF, random forest.

Nifedipine, Nitrendipine, Tamoxifen and Verapamil) out of nine intermediate and low TdP risk compounds, respectively, decreased the activity of cardiomyocytes at a concentration higher than ETPC (Figs. 3 and 4, Table SII). In addition, three (Amiodarone, Methadone and Nicotinamide) out of seven of the non-CiPA compounds decreased the cell activity of cardiomyocytes at concentrations greater than ETPC (Fig. 5).

BPM was used to evaluate the effect of compounds on the contractile function of the cardiomyocytes. Of the high TdP risk compounds, six out of eight lead to a decrease in BPM (Fig. 2). In addition, ibutilide, quinidine, sotalol and vandetanib all led to BPM decrease at concentrations less than ETPC. In the intermediate TdP risk compounds set, nine (Astemizole, Chlorpromazine, Cisapride, Clarithromycin, Droperidol, Ondansetron, Pimozide, Risperidone and Terfenadine) out of eleven were found to decrease BPM (Fig. 3, Table SII), with only domperidone concentration having been lower than ETPC. BPM was decreased by four (Diltiazem, Metoprolol, Mexiletine and Tamoxifen) out of nine low TdP risk compounds at concentrations greater than ETPC (Fig. 4, Table SII). Furthermore, four (Amiodarone, Moxifloxacin, Methadone and Nicotinamide) out of seven of the non-CiPA compounds decreased BPM at a concentration greater than ETPC, excluding nicotinamide (Fig. 5).

By contrast, two out of eight, two out of eleven and five out of nine compounds with high, intermediate and low TdP risk, respectively, led to increases in BPM (Figs. 2-4). In addition, the incidence of arrhythmia and FPDc prolongation was 57.89 and 84.21%, respectively, when BPM was decreased (Table II). Spearman correlation analysis showed that reducing BPM was significantly correlated with the occurrence of FPDc prolongation ( $\rho = 0.438$ ,  $P < 0.01$ ). However, the incidence of arrhythmia and FPDc prolongation were 66.67 and 44.44%, respectively (Table II), when BPM was increased. However, no relationship was noted between BPM increase, arrhythmia and FPDc prolongation.

**Effect of compounds on cardiomyocyte rhythm.** Of the high TdP risk compounds, seven (Azimilide, Bepridil, Disopyramide, Ibutilide, Quinidine, Sotalol and Vandetanib) out of eight were observed to induce arrhythmia-like waveforms (Table I). Similarly, ibutilide was observed to cause arrhythmia-like

Table I. Model predictors for all compounds tested.

TdP risk	Compounds	ETPC, $\mu\text{M}$	ETPC1	Arrhythmia-like Events	ETPC2	FPDc changes	%change in FPDc
H	Azimilide	$7.0 \times 10^{-2}$	$7.1 \times 10^{-1}$	1	$7.1 \times 10^{-1}$	1	35
H	Bepriidil	$3.2 \times 10^{-2}$	$3.1 \times 10^2$	1	$9.4 \times 10^{-1}$	3	-11
H	Disopyramide	$7.0 \times 10^{-1}$	$1.4 \times 10^{-1}$	1	$1.4 \times 10^{-1}$	1	65
H	Dofetilide	$2.0 \times 10^{-3}$	-	0	$1.5 \times 10^1$	1	30
H	Ibutilide	$1.0 \times 10^{-1}$	$1.0 \times 10^{-1}$	1	$1.0 \times 10^{-1}$	1	77
H	Quinidine	$3.0 \times 10$	$3.0 \times 10^{-2}$	1	$3.0 \times 10^{-2}$	1	33
H	Sotalol	$1.5 \times 10^1$	$2.0 \times 10$	1	$7.0 \times 10^{-2}$	1	59
H	Vandetanib	$3.0 \times 10^{-1}$	$3.0 \times 10^{-2}$	1	$3.3 \times 10^1$	1	53
I	Astemizole	$3.0 \times 10^{-4}$	$3.3 \times 10^2$	1	$3.3 \times 10$	1	50
I	Chlorpromazine	$3.5 \times 10^{-2}$	-	0	$8.7 \times 10^1$	1	57
I	Cisapride	$2.6 \times 10^{-3}$	-	0	$1.2 \times 10^3$	2	10
I	Clarithromycin	$1.2 \times 10$	-	0	$8.0 \times 10^{-2}$	3	-43
I	Clozapine	$7.1 \times 10^{-2}$	$1.4 \times 10^2$	1	$4.2 \times 10^{-1}$	1	65
I	Domperidone	$2.0 \times 10^{-2}$	$1.5 \times 10$	1	$1.5 \times 10^1$	1	45
I	Droperidol	$1.6 \times 10^{-2}$	$1.9 \times 10^1$	1	$6.3 \times 10$	1	38
I	Ondansetron	$3.7 \times 10^{-1}$	$8.1 \times 10^{-1}$	1	$8.1 \times 10$	2	9
I	Pimozide	$4.3 \times 10^{-4}$	$2.3 \times 10$	1	$2.3 \times 10$	1	49
I	Risperidone	$1.8 \times 10^{-3}$	$5.6 \times 10^2$	1	$5.6 \times 10^1$	1	35
I	Terfenadine	$2.9 \times 10^{-4}$	-	0	$3.5 \times 10^3$	2	10
L	Diltiazem	$1.3 \times 10^{-1}$	-	0	$2.3 \times 10^{-1}$	3	-16
L	Loratadine	$4.5 \times 10^{-4}$	-	0	$6.7 \times 10^1$	3	-19
L	Ranolazine	$1.9 \times 10$	$1.5 \times 10^1$	1	$5.1 \times 10^{-1}$	1	27
L	Metoprolol	$1.8 \times 10$	-	0	$6.0 \times 10^{-2}$	1	60
L	Mexiletine	$2.5 \times 10$	-	0	$1.2 \times 10$	2	10
L	Nifedipine	$7.7 \times 10^{-3}$	-	0	$1.3 \times 10^2$	3	-10
L	Nitrendipine	$3.0 \times 10^{-3}$	$3.3 \times 10^2$	1	$9.9 \times 10^{-1}$	3	-51
L	Tamoxifen	$2.1 \times 10^{-2}$	$1.4 \times 10^2$	1	$1.4 \times 10^1$	3	-46
L	Verapamil	$4.5 \times 10^{-2}$	-	0	-	0	0
Non	Amiodarone	$7.0 \times 10^{-4}$	-	0	$1.4 \times 10^4$	1	25
Non	Flecainide	$7.5 \times 10^{-1}$	$1.3 \times 10$	1	$1.3 \times 10^{-1}$	1	41
Non	Moxifloxacin	$3.6 \times 10$	-	0	$8.4 \times 10^1$	1	40
Non	E4031	$8.4 \times 10^{-3}$	-	0	$1.2 \times 10^{-1}$	3	-33
Non	Methadone	$9.9 \times 10^{-1}$	-	0	$2.0 \times 10^{-1}$	1	51
Non	Nicotinamide	$1.2 \times 10^3$	-	0	$4.0 \times 10^{-2}$	1	37
Non	Mannitol	$2.4 \times 10^3$	-	0	$2.0 \times 10^{-5}$	1	33

TdP, torsades de pointes; H, high; I, intermediate; L, low; Non, non-Comprehensive *in vitro* Proarrhythmia Assay; ETPC, effective therapeutic plasma concentration; ETPC1, drug concentration (folds over ETPC) when drug-induced arrhythmia-like events were first observed. Arrhythmia-like events an arrhythmia waveform was observed and recorded as 1, no arrhythmia waveform was recorded as 0. ETPC2, drug concentration (folds over ETPC) at which the FPDc change was observed. FPDc changes the type of FPDc change, 1  $\geq 30\%$ , 2  $\geq 10\%$ , 3  $< 0$ , 0=no change.

waveforms at 10% of the ETPC, which was the minimum multiple of the ETPC. Bepriidil induced arrhythmia-like waveforms at 312.5 times of the ETPC, which was the highest multiple of the ETPC. No arrhythmia-like waveforms were observed in dofetilide up to 150 times of the ETPC (Table I).

In the intermediate TdP risk compound group, seven (Astemizole, Clozapine, Domperidone, Droperidol, Ondansetron, Pimozide and Risperidone) out of eleven caused arrhythmia-like waveforms (Table I). Ondansetron induced

arrhythmia-like waveforms at 81% of the ETPC, which was the minimum multiple of the ETPC. In addition, arrhythmia-like waveforms were observed with risperidone at 555.6 times of the ETPC, which was the highest multiple times of the ETPC. For the other four compounds, no arrhythmia-like waveforms were observed at the tested concentrations (Table I).

Among the low TdP risk compounds, ranolazine, nitrendipine and tamoxifen were observed with arrhythmia-like waveforms at 15.4, 331.1 and 142.9 times of the ETPC, respectively. Only

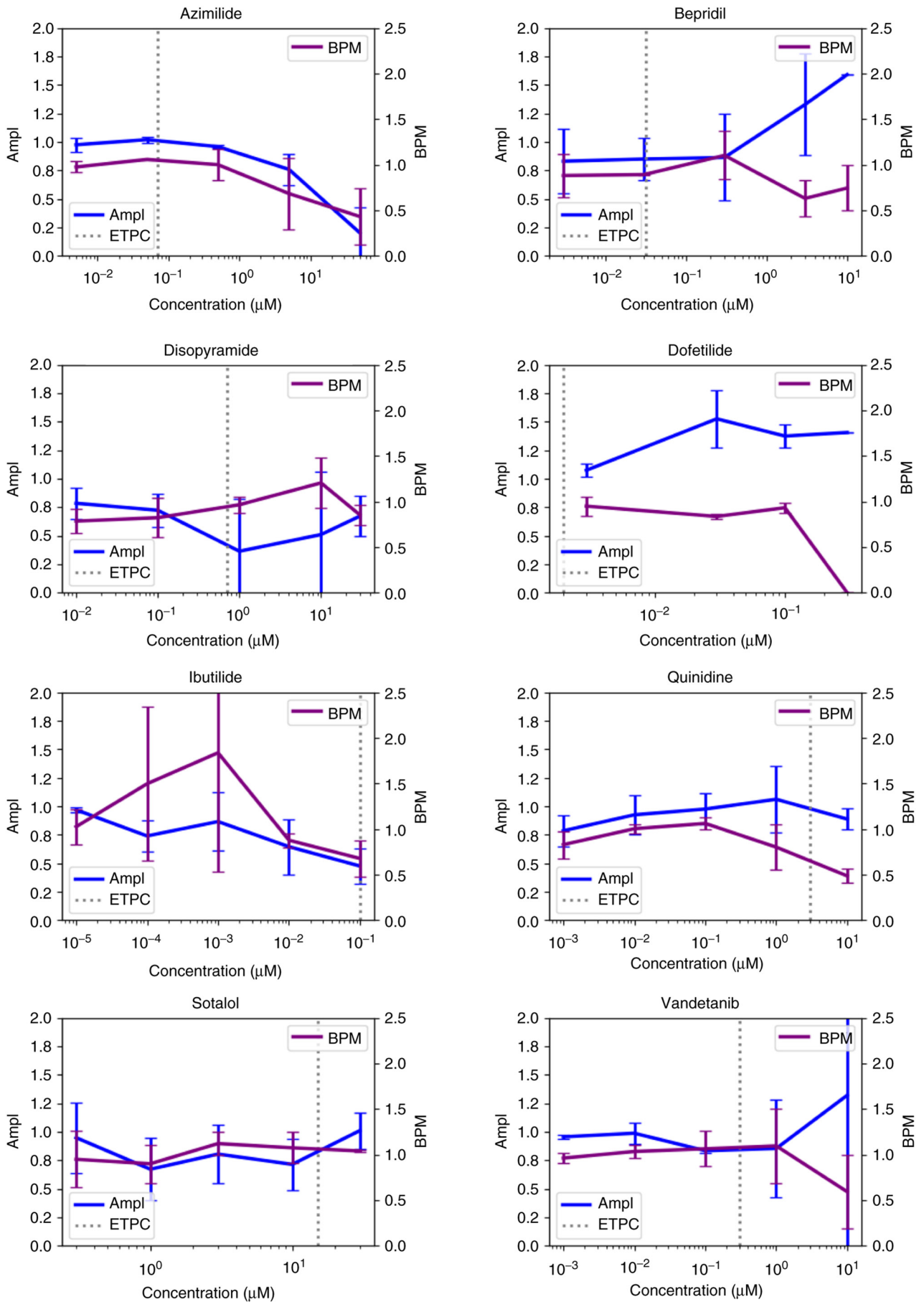


Figure 2. Effects of high torsades de pointes risk compounds on Ampl and BPM. Y-axis on the left represents the change in Ampl. Y-axis on the right represents the change in BPM. Concentrations are expressed on a logarithmic scale and the first data point is from zero concentration (0.1% DMSO). Ampl, amplitude; BPM, beats per minute; ETPC, effective therapeutic plasma concentration.

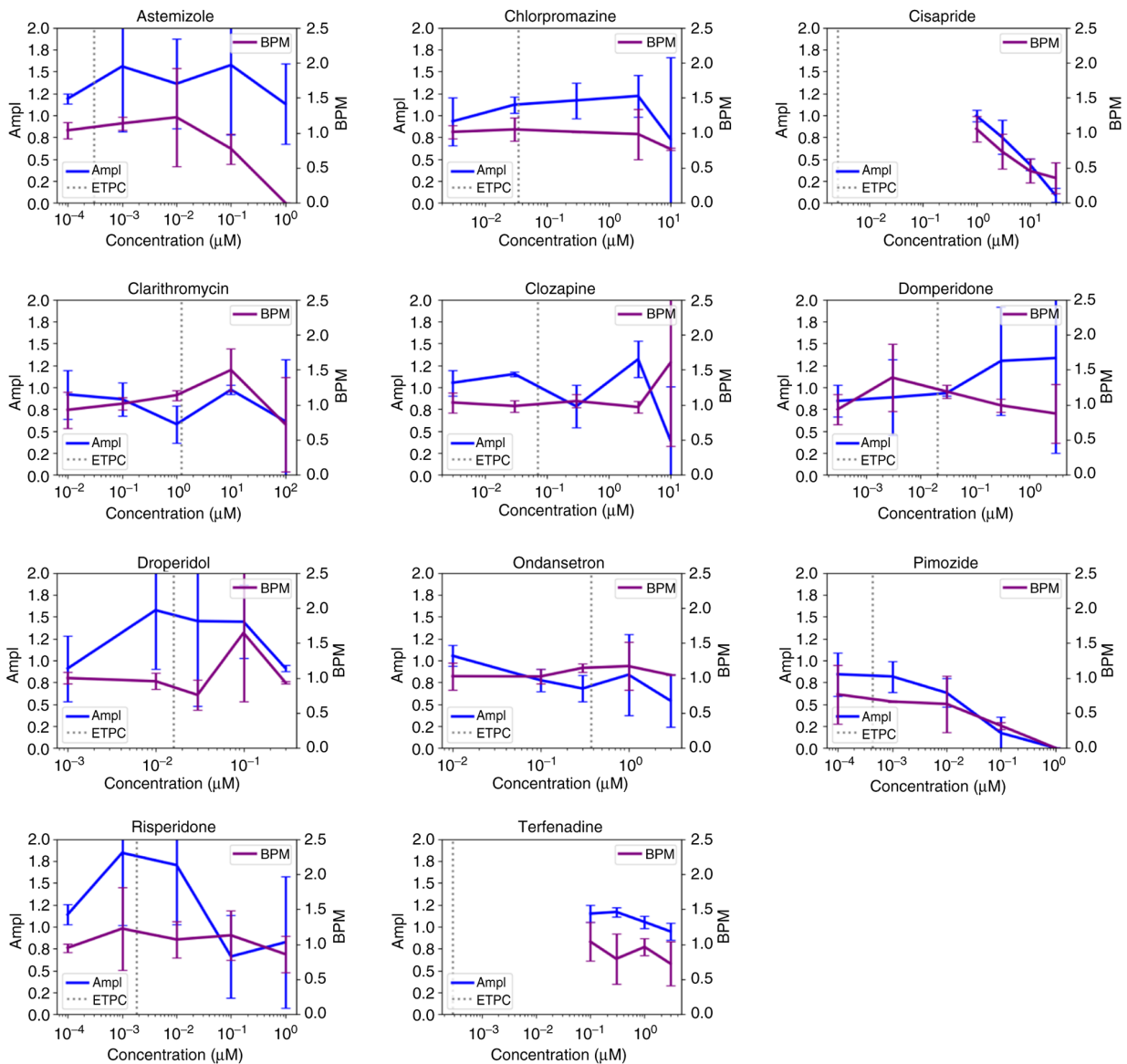


Figure 3. Effects of intermediate torsades de pointes risk compounds on Ampl and BPM. Y-axis on the left represents the change in Ampl. Y-axis on the right represents the change in BPM. Concentrations are expressed on a logarithmic scale and the first data point is from zero concentration (0.1% DMSO). Ampl, amplitude; BPM, beats per minute; ETPC, effective therapeutic plasma concentration.

flecainide was observed with arrhythmia-like waveforms at 1.33 times of the ETPC of the seven non-CiPA compounds, while no arrhythmia-like waveforms were observed in other compounds (Table I).

*Effect of compounds on FPDC of cardiomyocytes.* Only bepridil was observed to not induce FPDC prolongation among the eight high TdP risk compounds, with the other seven compounds showing FPDC prolongation in hiPSC-CMs after administration (Fig. 6, Table I), among which, dofetilide and vandetanib caused FPDC prolongation at concentrations higher than ETPC. Moreover, azimilide, disopyramide, ibutilide, quinidine and sotalol were observed with FPDC prolongation at concentrations lower than ETPC (Fig. S2).

Only clarithromycin had no FPDC prolongation among the eleven intermediate TdP risk compounds, while the remaining ten compounds were observed with FPDC prolongation (Fig. 6, Table I), of which, clozapine's concentration was 42% of the

ETPC. The other nine compounds' concentrations were higher compared with the ETPC (Fig. S3).

Among the nine compounds with low TdP risk, ranolazine (51% of the ETPC), metoprolol (6% of the ETPC) and mexiletine (1.2 times of the ETPC) could induce FPDC prolongation, while no FPDC prolongation was observed in the remaining six compounds (Figs. 6 and S4, Table I). The seven non-CiPA compounds, except for E4031, were all observed to cause FPDC prolongation (Figs. 6 and S5; Table I).

#### Model establishment and validation

*Model selection.* The classification accuracy of LR, SVM and DT was 0.86, 0.79 and 0.93, respectively, when the training set was used for modeling; the recall rates of these three models for intermediate- and high-risk compounds were 0.89, 0.74 and 0.89, respectively; and the AUC were 0.84, 0.81 and 0.95, respectively (Table SIII). The classification



Table II. Correlation of BPM with Arrhythmia-like Events and FPD prolongation

TdP risk	BPM changes	Number of Arrhythmia-like Events	Number of FPD prolongation
High	Reduced (n=6)	5	6
	Elevated (n=2)	2	1
Intermediate	Reduced (n=9)	5	8
	Elevated (n=2)	2	2
Low	Reduced (n=4)	1	2
	Elevated (n=5)	2	1
Proportion of Arrhythmia-like events due to reduced BPM			57.89%
Proportion of Arrhythmia-like events due to elevated BPM			66.67%
Proportion of FPD prolongation due to the reduced BPM			84.21%
Proportion of FPD prolongation due to the elevated BPM			44.44%

TdP, torsades de pointes.

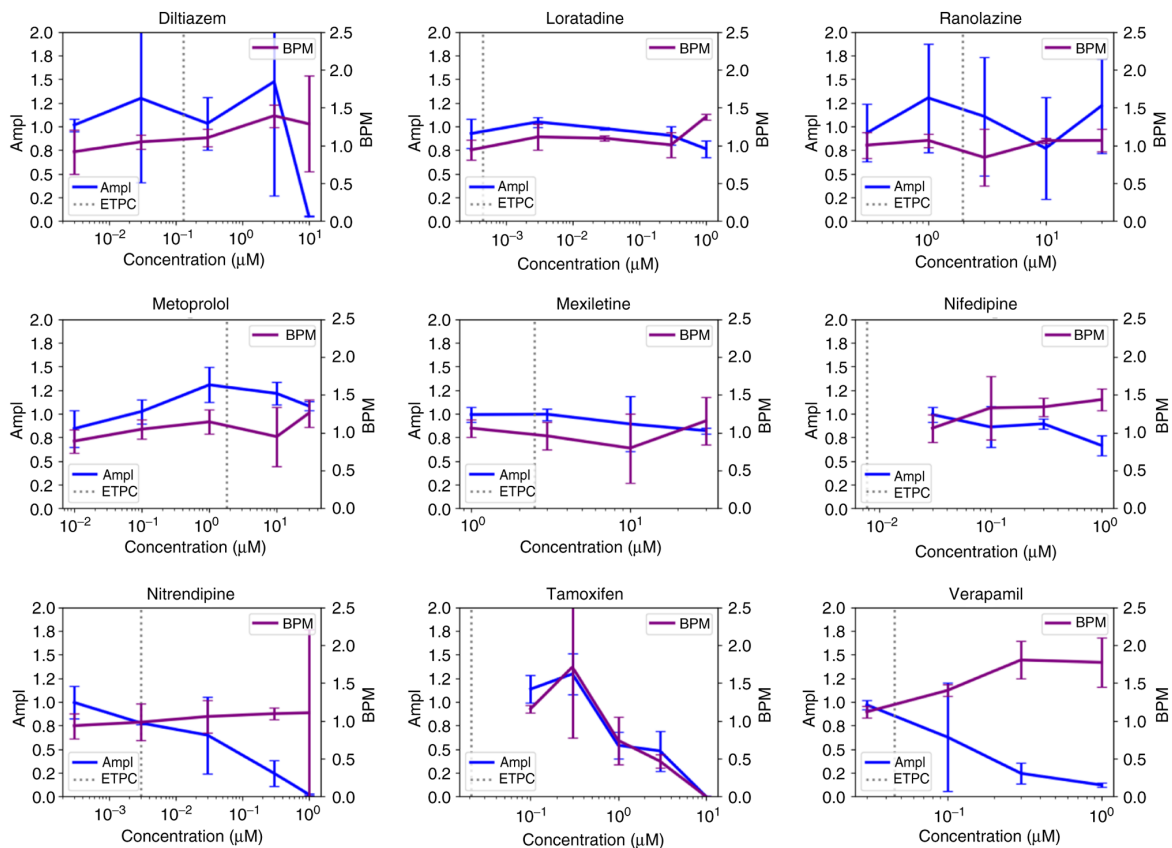


Figure 4. Effects of low torsades de pointes risk compounds on Ampl and BPM. Y-axis on the left represents the change in Ampl. Y-axis on the right represents the change in BPM. Concentrations are expressed on a logarithmic scale and the first data point is from zero concentration (0.1% DMSO). Ampl, amplitude; BPM, beats per minute; ETPC, effective therapeutic plasma concentration.

accuracy of KNN, AdaBoost, CatBoost and RF were all 1.00 and the recall rates in the training set were all 1.00, and all the AUC were 1.00 (Table SIII). According to the performance

of each model in the training and test sets (Table III), a high AUC value indicates a strong distinguishing ability of the model, while a small difference in AUC, observed between

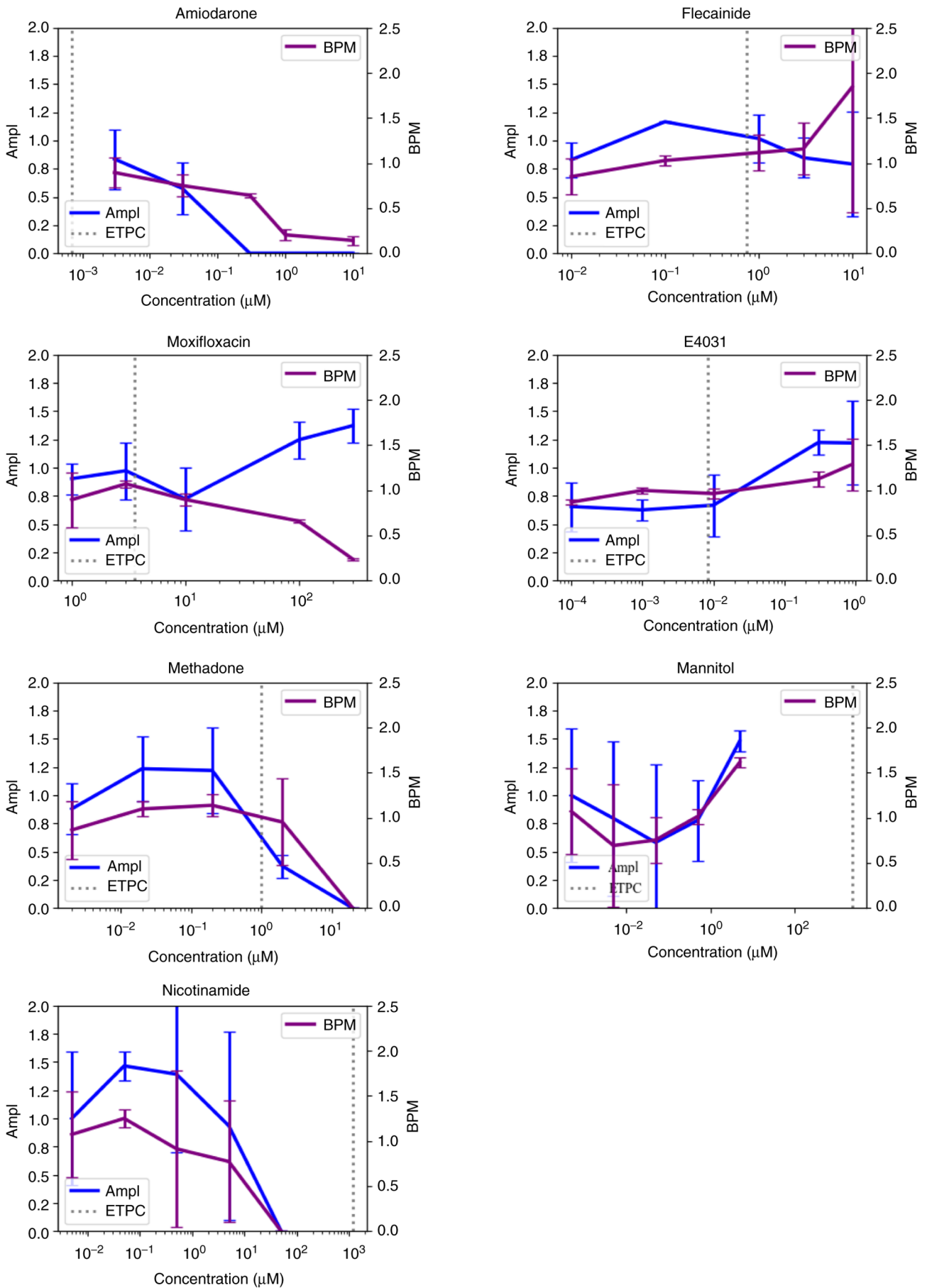


Figure 5. Effects of non-CiPA compounds on Ampl and BPM. Y-axis on the left represents the change in Ampl. Y-axis on the right represents the change in BPM. Concentrations are expressed on a logarithmic scale and the first data point is from zero concentration (0.1% DMSO). Ampl, amplitude; BPM, beats per minute; ETPC, effective therapeutic plasma concentration.



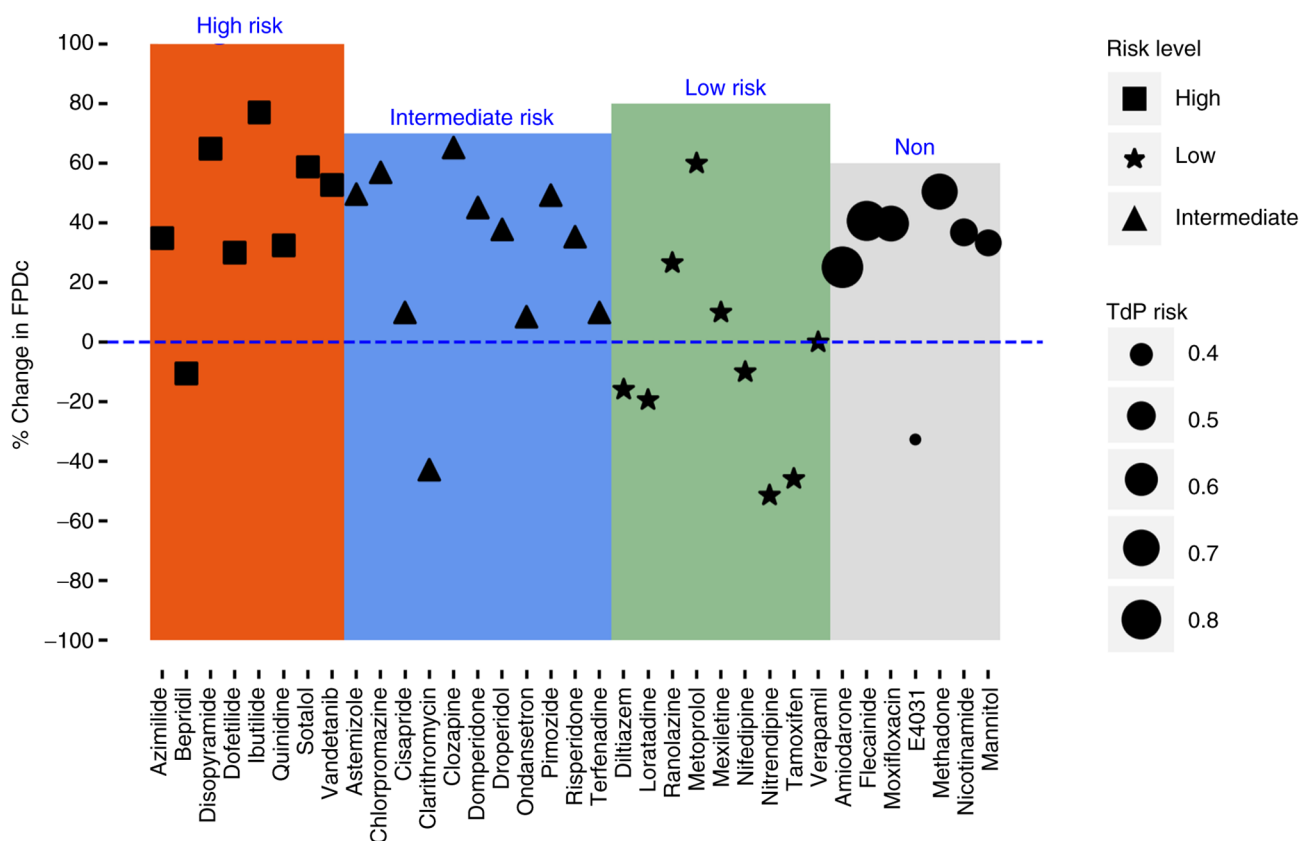


Figure 6. Changes in field potential of compounds with different TdP risk levels and non-CiPA compounds. Non-CiPA compound risk labels were predicted using the established voting classifier model. CiPA, Comprehensive *in vitro* Proarrhythmia Assay; TdP, torsades de pointes; FPDc, corrected field potential duration.

the training and the test sets, indicates good model stability. According to the discriminative ability and stability, LR and AdaBoost were the two models with best performance in both the training and test sets and were selected as sub-models going forward. Each sub-model is assigned a similar weight and the new prediction model (VC model) is established through soft voting.

**Model predictors evaluation.** Arrhythmia-like waveforms and FPDc prolongation the two most important modelling indicators. Spearman correlation analysis showed that arrhythmia-like waveforms were correlated with the predictive values ( $r=0.40$ ,  $P<0.05$ , data not shown). Pearson correlation analysis showed that FPDc prolongation was also significantly correlated with the predictive values ( $r=0.744$ ,  $P<0.001$ , data not shown).

**Model evaluation.** The newly established VC model was compared with the LR and AdaBoost models. The LR and AdaBoost models both performed poorly on the training and test sets (Fig. 7, Table IV). However, the VC model performed well in both the training and test sets. Only a small difference was noted in all the parameters between the two sets, indicating that the VC model had good stability.

**Threshold setting.** The default threshold of intermediate and high to low risk was 0.5 in the process of model establishment. When the threshold was set as 0.5, clarithromycin at intermediate-risk was predicted to be low-risk and ranolazine (low-risk) was predicted to be an intermediate- or high-risk compound with a consistency of 92.8% (Fig. 8). In the test

set, amiodarone, flecainide, moxifloxacin and methadone were all predicted to be of intermediate or high-risk, while E4031, nicotinamide and mannitol were low risk with a consistency of 100% (Fig. 8).

## Discussion

Primary rat cardiomyocytes are currently the main cellular model for cardiac toxicity evaluation (30). However, pronounced differences in species have been noted between mice and humans, resulting in 37% tolerance of compounds in mice, which was 10 times higher compared with that of humans (31). Increasing attention has highlighted the advantages of hiPSC-CMs in previous studies. Moreover, hiPSC-CMs express various human cardiac ion channels and genes encoding key components of the  $Ca^{2+}$  cycle, which greatly reduces the impact of differences between species and reduces the discrepancy between rat and adult primary human cardiomyocytes (32-34). hiPSC-CMs display the complex physiological functions associated with human myocardial cells *in vitro* and possess the biochemical and molecular biological characteristics of human cardiac myocytes. Moreover, hiPSC-CMs are easy to purify and can be cultured *in vitro* for extended periods of time compared to rat primary cardiomyocytes (data not shown). Hence, it is an excellent model for *in vitro* prediction of arrhythmia *in vivo*. In the present study, hiPSC-CMs has a clonal morphology and gene expression that highly resembles

Table III. AUC results of seven models.

Sample set	LR	SVM	KNN	DT	AdaBoost	CatBoost	RF
Training set	0.84	0.81	1.00	0.95	1.00	1.00	1.00
Test set	0.83	0.75	0.71	0.50	0.83	0.71	0.83

LR, logistic regression; SVM, support vector machine; KNN,  $k$ -nearest neighbor algorithm; DT, decision tree; AdaBoost, adaptive boosting; RF, random forest.

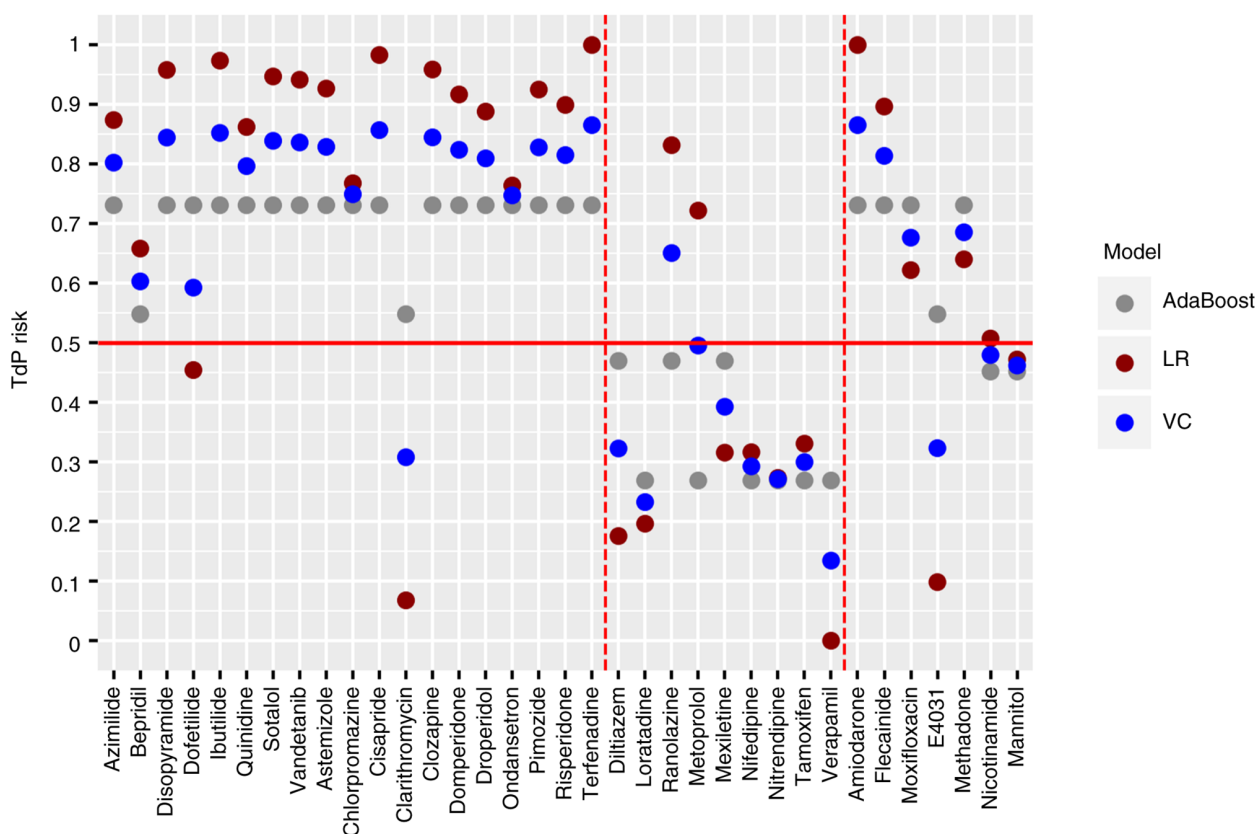


Figure 7. Predicted TdP risk for all compounds using LR, AdaBoost and VC models. TdP, torsades de pointes; LR, logistic regression; AdaBoost, adaptive boosting; VC, voting classifier.

human embryonic stem cells. It is probable that different hiPSC-CM lines can behave differently in response to electrophysiological changes, so three hiPSC-CM lines were evaluated in previous studies. The prolongation of FPDC was used as a single predictor for the TdP risk, showing the sensitivity and specificity of the hiPSC-CM line from Cellapy were optimal, as such this cell line was selected for further investigations.

The effects of different compounds on cell activity, which aimed to observe cytotoxicity and the rationality of dose design, were evaluated in the present study. Ampl also reflects the beating pattern of the hiPSC-CMs and the change in beating patterns reflects which ion channels in the cell membrane are affected (35). The results showed that no cytotoxicity was noted at all concentrations of the compounds (Table SI), but the correlation between the change of Ampl and TdP risk needs further evaluation. Simultaneously, the effects of compounds on the BPM of cardiomyocytes were tested.

Abnormal heart rate correlates with drug-induced cardiotoxicity (36). According to the present data, compounds that inhibited the contractile function of cardiomyocytes resulted in reduced BPM, which is more likely to cause arrhythmia and more likely to induce prolonged FPDC. This suggested that inhibition of cell beating may be a risk factor for TdP.

Drug effects and adverse reactions are closely related to dose, for some compounds, the risk of side effects can increase with increasing dose, ETPC is usually proportional to the dose, and is a common indicator of the dose administered (37). Thus, ETPC was also accepted as a model predictor. The arrhythmia-like waveforms are another important model predictor. Arrhythmia-like waveforms were observed in all three TdP risk compound groups and high-risk compounds were more likely to induce arrhythmia-like waveforms. A notable event, which advises compound risk prediction, is the possibility of increased TdP if arrhythmia-like waveforms appeared at a dose lower than the ETPC.

Table IV. Model evaluation results.

Model	Training set			Test set		
	Accuracy	Recall	AUC	Accuracy	Recall	AUC
LR	0.86	0.89	0.84	0.86	1.00	0.83
AdaBoost	1.00	1.00	1.00	0.86	1.00	0.83
VC	0.93	0.95	0.92	1.00	1.00	1.00

AUC, area under the curve; LR, logistic regression; AdaBoost, adaptive boosting; VC, voting classifier.

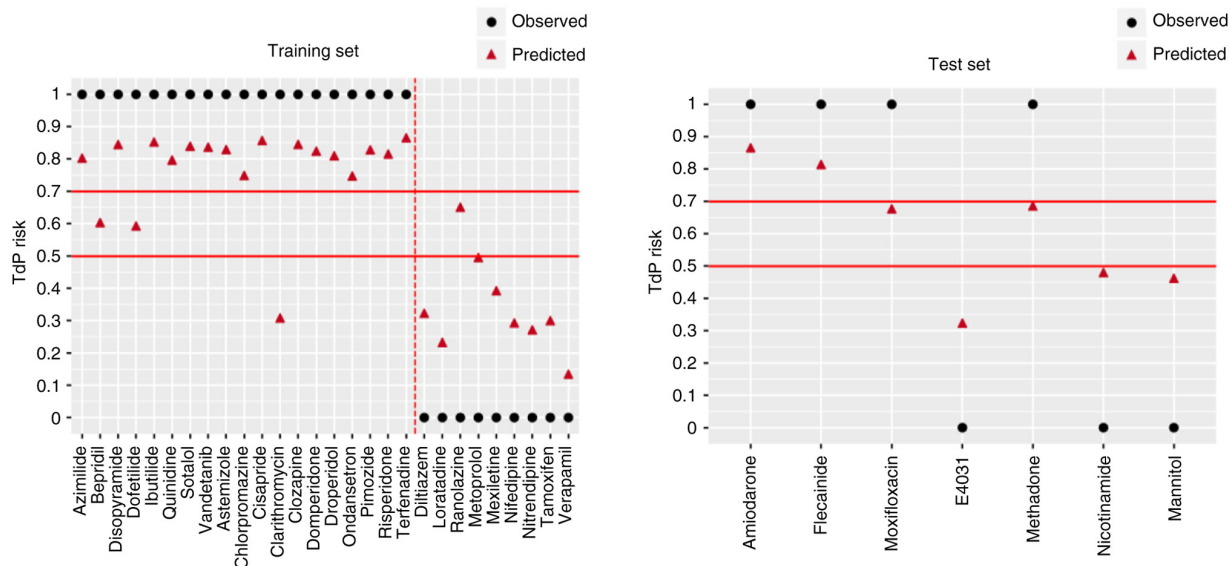


Figure 8. Consistency between the predicted value of the VC model and the actual observed value. The observed results were retrieved from the Comprehensive *in vitro* Proarrhythmia Assay program or other published literature. TdP, torsades de pointes; VC, voting classifier.

AP detection is based on individual cardiomyocytes and in this context there is a lack intercellular communication, so instead small populations cardiomyocytes were chosen (38). Instead of recording individual APs and early depolarization, the CardioExcyte 96 recorded field potential. FPdc prolongation was considered to be closely related to TdP occurrence. In the multi-electrode array (MEA) test, adjacent recording electrodes can record spontaneous APs of the cell population as external field potential. The recording electrode can monitor the change in field potential when an AP spreads across monolayer cells (39). Halbach *et al* (40) revealed a direct relationship between the rise in time of APs and field potentials, showing that APs and field potentials are linearly correlated. In the present study, FPdc change was observed to be consistent with instances of arrhythmia, with the higher the FPdc prolongation probability, the higher the risk of TdP. Arrhythmia-like events and the type of FPdc change were the most important among the six predictors. Though no FPdc prolongation was observed for bepridil and clarithromycin in the present study, thus, they were classified as low-risk compounds; no arrhythmia-like events were observed during administration of dofetilide, so dofetilide was also classified as a low-risk compound.

Sharifi *et al* (41) developed a TdP prediction model based on the chemical structure of the compounds, though this model

works only if compounds with similar structures possess the same electrophysiological responses. Additionally, the drugs' effects on different ion channels have also been used as predictors for TdP risk (42). However, previous studies of TdP prediction models have mainly been based on the electrophysiological effects of compounds on hiPSC-CMs. The classical models for predicting TdP risk based on hiPSC-CMs mainly include the LR model (43). However, in the current study, its classification accuracy was only 0.86 and the recognition rate of intermediate- and high-risk compounds was only 0.89, which showed that the model classification ability was not sufficient. Blinova *et al* (21) used the LR model to assess the risk of dysrhythmia, one high-risk compound (bepridil) and four intermediate-risk compounds (risperidone, terfenadine, chlorpromazine and clozapine) were incorrectly predicted to be low-risk; this indicated that the logical regression classifier may not be able to identify some significant nonlinear relationships and detect the correlation between predictive variables, making it prone to false negatives in practical application (22).

In the current study, the classification accuracy, the recall rate and the AUC of KNN, CatBoost and RF were all 1.00 in the training set, but these models performed poorly in the test set. Thus, these models may be overfitted. The main influencing

factors of overfitting may include small sample size in the training set and the inconsistency of data distribution in the training and test sets (44). The difference between data distribution may have introduced bias into the models. Considering that a precise classification is difficult to achieve with only one model, the combination of multiple models was used in the current study. Thus, LR and AdaBoost (a black box model widely used in computer-aided diagnosis), were chosen as the sub-models according to the classification performance of each model (45). Finally, a new model named VC was established through a soft voting strategy. The AUC of the VC model had little difference between training set and test set and the consistency of the VC model between the predicted and observed results was optimal. This suggested that this model could tolerate a certain degree of differential data distribution through the soft voting strategy.

Moreover, 28 CiPA compounds were considered to be a small sample size (46). The data showed that AdaBoost had improved performance compared with VC in the training set, but VC outperformed AdaBoost in the test set. Whether data distribution of an unknown compound is consistent with the training set is unknown, thus the soft voting strategy was used and the VC model was chosen to avoid overfitting and enhance the generalization of the model.

The prediction results of VC for the training set of 28 known compounds showed that bepridil, dofetilide and clarithromycin were classified as a low-risk at a threshold of 0.7, but bepridil and dofetilide are high TdP risk compounds, which can cause QT interval prolongation and induce TdP (47,48). In the present study, bepridil was predicted as a low-risk compound owing to no FPDC prolongation was observed. Bepridil is a calcium antagonist and also blocks sodium and potassium channels, so the effect of potassium channel blocking may be counterbalanced by calcium channel blocking (49). This may be one of the reasons for the shortening of its FPDC. No arrhythmia-like waveforms were observed in dofetilide, which may be the main reason why this compound was predicted to be low-risk. The minimum and maximum concentrations of dofetilide were 0.03 (15 times of the ETPC) and 0.3  $\mu\text{M}$  (150 times of the ETPC), respectively. The cells stopped beating at the maximum concentration, thus, the concentrations used may have been inappropriate and further experimental confirmation is required.

Clarithromycin is an intermediate-risk compound and an hERG channel blocker (50). No QT prolongation was found in healthy individuals after clarithromycin administration (51). However, women, the elderly and patients with underlying heart disease may exhibit increased QTc prolongation and increased risk of TdP induced by clarithromycin (52). In the present study, FPDC showed shortening after clarithromycin administration and was predicted as low risk. Ando *et al.* (17) reported that clarithromycin at 13 times (42.9  $\mu\text{M}$ ) of the free plasma concentration can lead to 10% FPDC prolongation. The experiment for clarithromycin was repeated in triplicate and no FPDC prolongation was observed at the highest concentration of 100  $\mu\text{M}$ , therefore, experimentation should be continued for verification.

According to the prediction results with 0.7 as the threshold, amiodarone and flecainide, both known compounds with associated TdP risk, were predicted to be high- or intermediate-risk compounds. Amiodarone is a class III antiarrhythmic drug, which can inhibit the hERG channel and cause QT prolongation (53). The TdP incidence of amiodarone

~15% after intravenous administration (54). Flecainide is a class IC antiarrhythmic drug, which can inhibit  $\text{K}^+$  channels, causing prolonged QT interval and TdP (55). According to the established model, the prediction results of amiodarone and flecainide are consistent with literature reports.

The risk threshold was adjusted to 0.5 because numerous false negatives were noted in the training set at 0.7 threshold value. Clarithromycin should be predicted as a high- or intermediate-risk compound, and ranolazine should be predicted as a low-risk compound, so clarithromycin was not identified and ranolazine was misidentified in the training set. However, amiodarone, flecainide, moxifloxacin and methadone in the test set were all correctly predicted to be high or intermediate risk compounds, while E4031, nicotinamide and mannitol were all predicted to have low-risk compounds. Tisdale (53) previously reported moxifloxacin to have known TdP risk, which supports the findings of the present study. Moxifloxacin is more prone to TdP in patients with multiple risk factors for prolonged QT interval (56). Methadone is also high risk at low doses and has the potential to prolong QT interval and develop TdP (57). E4031 is an hERG blocker that can prolong QT interval (58). However, to the best of our knowledge, no clinical report has been on the risk of E4031-induced TdP. Nicotinamide and mannitol had not been reported to induce TdP risk. Therefore, the consistency between the predicted and the observed results was 92.8 and 100% in the training and test sets, respectively, when 0.5 was used as the threshold value. In toxicity evaluation, false positives could be supported by other experiments, while false negatives could cause serious clinical risks. Thus, the low false-negative value of 0.5 was chosen as the threshold value.

A number of uncertainties have been noted in extrapolating animal data to humans in the nonclinical safety evaluations of new drugs and remains a troubling issue in toxicity research (59). Thus, hiPSC-CMs are a viable way to reduce uncertainty caused by species differences. As such, the false positive and false negative rates in toxicity evaluation caused by a single predictor was avoided in the present study. The prediction model was able to reveal the relationship between prediction indicators and results based on the specific algorithms. Each model had its advantages in a particular sample set, though the two models with improved performance were selected to establish a new model. Thus, avoiding the defects of a single model methodology and improving the prediction accuracy and stability of the model.

Though a functional TdP prediction model was established based on hiPSC-CMs in the present study, data was generated from only a single cell batch. Hence, assessing the differentiation variability and reproducibility of this model is still necessary. Although hiPSC-CMs are considered an improvement on rodent cells, this type of CMs bear more resemblance to neonatal CMs or those in early development rather than adult CMs, and their functional and electrophysiological properties are not fully mature, so there are still some limitations in their application (60). In the present study, small sample size was used for both training and test sets and no risk labels were assigned to the test set, which is inconsistent with the training set. These two factors may have led to over-fitting of the models. Thus, expanding the sample size for further verification is needed in future investigations. Additionally, consistent dataset risk labels are needed and 'Transfer learning' may

also be useful to overcome differences in data distribution, for small data sets, transfer learning is a useful strategy to increase model power for specific tasks (61).

In the present study, a normal cell model was used, therefore, it is mainly applicable to the prediction of TdP in healthy patients after drug treatment or during treatment. For specific clinical contexts, such as patients with long QT syndrome, a disease model cell line should be used as the research subject to establish a risk prediction model for TdP. In total, 28 compounds were used to establish the TdP risk prediction model based on hiPSC-CMs. LR and AdaBoost were taken as sub-models, with the same assigned weight, to create a new TdP risk prediction model using a soft voting strategy. This improved upon the accuracy of the individual models and enhanced the generalization ability. In the established TdP risk prediction model, 0.5 was set as the threshold of TdP risk. All the seven compounds in the test sets were accurately classified, achieving good consistency. The current study also found that the multiple compounds inhibited the beating of cardiomyocytes and those with reduced beating frequency were more likely to have arrhythmic waveforms and more likely to induce prolonged FPDCs.

### Acknowledgements

The authors would like to thank Dr Gaojian Cheng (National Institutes for Food and Drug Control, Beijing, China) for technical guidance and Dr Hong Zhi Zhang (National Institutes for Food and Drug Control) for statistical analysis. The authors would also like to thank Dr Yu Chang and Professor Feng Lan (Chinese Academy of Medical Sciences & Peking Union Medical College, Beijing, China) for language editing.

### Funding

This work was supported by the National Major Scientific and Technological Special Project for 'Significant New Drugs Development' (grant no. 2018ZX09201017-001) from the Ministry of Science and Technology of the People's Republic of China.

### Availability of data and materials

The datasets used and/or analyzed during the current study are available from the corresponding author on reasonable request

### Authors' contributions

DP, SW and BL contributed to the conception of the study. DP and SW conducted the experiments. DP analyzed data and wrote the manuscript. DP and SW confirm the authenticity of all the raw data. All authors have read and approved the final manuscript.

### Ethics approval and consent to participate

Not applicable.

### Patient consent for publication

Not applicable.

### Competing interests

The authors declare that they have no competing interests.

### References

1. Frommeyer G and Eckardt L: Drug-induced proarrhythmia: Risk factors and electrophysiological mechanisms. *Nat Rev Cardiol* 13: 36-47, 2016.
2. Vicente J, Zusterzeel R, Johannesen L, Mason J, Sager P, Patel V, Matta MK, Li ZH, Liu J, Garnett C, *et al*: Mechanistic model-informed proarrhythmic risk assessment of drugs: Review of the 'CiPA' initiative and design of a prospective clinical validation study. *Clin Pharmacol Ther* 103: 54-66, 2018.
3. Niemeijer MN, van den Berg ME, Eijgelsheim M, Rijnbeek PR and Stricker BH: Pharmacogenetics of drug-induced QT interval prolongation: An update. *Drug Saf* 38: 855-867, 2015.
4. El-Sherif N and Turitto G: Electrolyte disorders and arrhythmogenesis. *Cardiol J* 18: 233-245, 2011.
5. Shah RR: Drugs, QT interval prolongation and ICH E14: The need to get it right. *Drug Saf* 28: 115-125, 2005.
6. Darpo B and Ferber G: The new S7B/E14 question and answer draft guidance for industry: Contents and commentary. *J Clin Pharmacol* 61: 1261-1273, 2021.
7. Vargas HM, Rolf MG, Wisialowski TA, Achanzar W, Bahinski A, Bass A, Benson CT, Chaudhary KW, Couvreur N, Dota C, *et al*: Time for a fully integrated nonclinical-clinical risk assessment to streamline QT prolongation liability determinations: A pharma industry perspective. *Clin Pharmacol Ther* 109: 310-318, 2021.
8. Sanguinetti MC and Mitcheson JS: Predicting drug-hERG channel interactions that cause acquired long QT syndrome. *Trends Pharmacol Sci* 26: 119-124, 2005.
9. Gintant G, Sager PT and Stockbridge N: Evolution of strategies to improve preclinical cardiac safety testing. *Nat Rev Drug Discov* 15: 457-471, 2016.
10. Zhang S, Zhou Z, Gong Q, Makielski JC and January CT: Mechanism of block and identification of the verapamil binding domain to HERG potassium channels. *Circ Res* 84: 989-998, 1999.
11. Fenichel RR, Malik M, Antzelevitch C, Sanguinetti M, Roden DM, Priori SG, Ruskin JN, Lipicky RJ, Cantilena LR and Independent Academic Task Force: Drug-induced torsades de pointes and implications for drug development. *J Cardiovasc Electrophysiol* 15: 475-495, 2004.
12. Yim DS: Five years of the CiPA project (2013-2018): What did we learn? *Transl Clin Pharmacol* 26: 145-149, 2018.
13. Park JS, Jeon JY, Yang JH and Kim MG: Introduction to in silico model for proarrhythmic risk assessment under the CiPA initiative. *Transl Clin Pharmacol* 27: 12-18, 2019.
14. Wallis R, Benson C, Darpo B, Gintant G, Kanda Y, Prasad K, Strauss DG and Valentin JP: CiPA challenges and opportunities from a non-clinical, clinical and regulatory perspectives. An overview of the safety pharmacology scientific discussion. *J Pharmacol Toxicol Methods* 93: 15-25, 2018.
15. Roden DM: Predicting drug-induced QT prolongation and torsades de pointes. *J Physiol* 594: 2459-2468, 2016.
16. Crestani T, Steichen C, Neri E, Rodrigues M, Fonseca-Alaniz MH, Ormrod B, Holt MR, Pandey P, Harding S, Ehler E and Krieger JE: Electrical stimulation applied during differentiation drives the hiPSC-CMs towards a mature cardiac conduction-like cells. *Biochem Biophys Res Commun* 533: 376-382, 2020.
17. Ando H, Yoshinaga T, Yamamoto W, Asakura K, Uda T, Taniguchi T, Ojima A, Shinkyo R, Kikuchi K, Osada T, *et al*: A new paradigm for drug-induced torsadogenic risk assessment using human iPSC cell-derived cardiomyocytes. *J Pharmacol Toxicol Methods* 84: 111-127, 2017.
18. Huo J, Wei F, Cai C, Lyn-Cook B and Pang L: Sex-related differences in drug-induced QT prolongation and torsades de Pointes: A new model system with human iPSC-CMs. *Toxicol Sci* 167: 360-374, 2019.
19. da Rocha AM, Creech J, Thonn E, Mironov S and Herron TJ: Detection of drug-induced torsades de Pointes arrhythmia mechanisms using hiPSC-CM syncytial monolayers in a high-throughput screening voltage sensitive dye assay. *Toxicol Sci* 173: 402-415, 2020.
20. Raphael F, De Korte T, Lombardi D, Braam S and Gerbeau JF: A greedy classifier optimization strategy to assess ion channel blocking activity and pro-arrhythmia in hiPSC-cardiomyocytes. *PLoS Comput Biol* 16: e1008203, 2020.



21. Blinova K, Dang Q, Millard D, Smith G, Pierson J, Guo L, Brock M, Lu HR, Kraushaar U, Zeng H, *et al*: International multisite study of human-induced pluripotent stem cell-derived cardiomyocytes for drug proarrhythmic potential assessment. *Cell Rep* 24: 3582-3592, 2018.
22. Tu JV: Advantages and disadvantages of using artificial neural networks versus logistic regression for predicting medical outcomes. *J Clin Epidemiol* 49: 1225-1231, 1996.
23. Heo J, Yoon JG, Park H, Kim YD, Nam HS and Heo JH: Machine learning-based model for prediction of outcomes in acute stroke. *Stroke* 50: 1263-1265, 2019.
24. Sherazi SW, Bae JW and Lee JY: A soft voting ensemble classifier for early prediction and diagnosis of occurrences of major adverse cardiovascular events for STEMI and NSTEMI during 2-year follow-up in patients with acute coronary syndrome. *PLoS One* 16: e0249338, 2021.
25. Asakura K, Hayashi S, Ojima A, Taniguchi T, Miyamoto N, Nakamori C, Nagasawa C, Kitamura T, Osada T, Honda Y, *et al*: Improvement of acquisition and analysis methods in multi-electrode array experiments with iPSC cell-derived cardiomyocytes. *J Pharmacol Toxicol Methods* 75: 17-26, 2015.
26. Gerds TA, Cai T and Schumacher M: The performance of risk prediction models. *Biom J* 50: 457-479, 2008.
27. Pencina MJ and D'Agostino RB Sr: Evaluating discrimination of risk prediction models: The C statistic. *JAMA* 314: 1063-1064, 2015.
28. Alba AC, Agoritsas T, Walsh M, Hanna S, Iorio A, Devereaux PJ, McGinn T and Guyatt G: Discrimination and calibration of clinical prediction models: Users' guides to the medical literature. *JAMA* 318: 1377-1384, 2017.
29. Ziegler R, Häusermann F, Kirchner S and Polonchuk L: Cardiac safety of kinase inhibitors-improving understanding and prediction of liabilities in drug discovery using human stem cell-derived models. *Front Cardiovasc Med* 8: 639824, 2021.
30. Harary I and Farley B: In vitro studies of single isolated beating heart cells. *Science* 131: 1674-1675, 1960.
31. Price PS, Keenan RE and Swartout JC: Characterizing interspecies uncertainty using data from studies of anti-neoplastic agents in animals and humans. *Toxicol Appl Pharmacol* 233: 64-70, 2008.
32. Sheng CC, Amiri-Kordestani L, Palmby T, Force T, Hong CC, Wu JC, Croce K, Kim G and Moslehi J: 21st century cardiology: Identifying cardiac safety signals in the era of personalized medicine. *JACC Basic Transl Sci* 1: 386-398, 2016.
33. Haraguchi Y, Ohtsuki A, Oka T and Shimizu T: Electrophysiological analysis of mammalian cells expressing hERG using automated 384-well-patch-clamp. *BMC Pharmacol Toxicol* 16: 39, 2015.
34. Higa A, Hoshi H, Yanagisawa Y, Ito E, Morisawa G, Imai JI, Watanabe S and Takagi M: Evaluation system for arrhythmogenic potential of drugs using human-induced pluripotent stem cell-derived cardiomyocytes and gene expression analysis. *J Toxicol Sci* 42: 755-761, 2017.
35. Abassi YA, Xi B, Li N, Ouyang W, Seiler A, Watzele M, Kettenhofen R, Bohlen H, Ehlich A, Kolossov E, *et al*: Dynamic monitoring of beating periodicity of stem cell-derived cardiomyocytes as a predictive tool for preclinical safety assessment. *Br J Pharmacol* 165: 1424-1441, 2012.
36. Wang SY, Wang XJ and Ma J: Progress in real time xCELLigence analysis system on drug cardiotoxicity screening. *Chin J Pharmacol Toxicol*, 27: 908-912, 2013.
37. Yue Peng, Ying BB, He Min and Yang ChaoWen: Study on hepatotoxicity of different doses of cisplatin in rats. *J Toxicol*, 33: 302-306, 2019.
38. Marcu IC, Illaste A, Heuking P, Jaconi ME and Ullrich ND: Functional characterization and comparison of intercellular communication in stem cell-derived cardiomyocytes. *Stem Cells* 33: 2208-2218, 2015.
39. Clements M: Multielectrode array (MEA) assay for profiling electrophysiological drug effects in human stem cell-derived cardiomyocytes. *Curr Protoc Toxicol* 68: 22.24.21-22.24.32, 2016.
40. Halbach M, Egert U, Hescheler J and Banach K: Estimation of action potential changes from field potential recordings in multicellular mouse cardiac myocyte cultures. *Cell Physiol Biochem* 13: 271-284, 2003.
41. Sharifi M, Buzatu D, Harris S and Wilkes J: Development of models for predicting Torsade de Pointes cardiac arrhythmias using perceptron neural networks. *BMC Bioinformatics* 18 (Suppl 4): S497, 2017.
42. Liu H, Ji M, Luo X, Shen J, Huang X, Hua W, Jiang H and Chen K: New p-methylsulfonamido phenylethylamine analogues as class III antiarrhythmic agents: Design, synthesis, biological assay, and 3D-QSAR analysis. *J Med Chem* 45: 2953-2969, 2002.
43. Chamberlain AM, Boyd CM, Manemann SM, Dunlay SM, Gerber Y, Killian JM, Weston SA and Roger VL: Risk factors for heart failure in the community: Differences by age and ejection fraction. *Am J Med* 133: e237-e248, 2020.
44. Belkin M, Hsu D, Ma S and Mandal S: Reconciling modern machine-learning practice and the classical bias-variance trade-off. *Proc Natl Acad Sci USA* 116: 15849-15854, 2019.
45. Hatwell J, Gaber MM and Atif Azad RM: Ada-WHIPS: Explaining AdaBoost classification with applications in the health sciences. *BMC Med Inform Decis Mak* 20: 250, 2020.
46. Kanda Y, Yamazaki D, Osada T, Yoshinaga T and Sawada K: Development of torsadogenic risk assessment using human induced pluripotent stem cell-derived cardiomyocytes: Japan iPSC cardiac safety assessment (JiCSA) update. *J Pharmacol Sci* 138: 233-239, 2018.
47. Aktas MK, Shah AH and Akiyama T: Dofetilide-induced long QT and torsades de pointes. *Ann Noninvasive Electrocardiol* 12: 197-202, 2007.
48. Jaiswal A and Goldberg S: Dofetilide induced torsade de pointes: Mechanism, risk factors and management strategies. *Indian Heart J* 66: 640-648, 2014.
49. Thomine S, Zimmerman S, Duijn BV, Barbier-Brygoo H and Guern J: Calcium channel antagonists induce direct inhibition of the outward rectifying potassium channel in tobacco protoplasts. *FEBS Lett* 340: 45-50, 1994.
50. Duncan RS, Ridley JM, Dempsey CE, Leishman DJ, Leaney JL, Hancox JC and Witchel HJ: Erythromycin block of the HERG K+ channel: Accessibility to F656 and Y652. *Biochem Biophys Res Commun* 341: 500-506, 2006.
51. van Haarst AD, van 't Klooster GA, van Gerven JM, Schoemaker RC, van Oene JC, Burggraaf J, Coene MC and Cohen AF: The influence of cisapride and clarithromycin on QT intervals in healthy volunteers. *Clin Pharmacol Ther* 64: 542-546, 1998.
52. Vieweg WV, Hancox JC, Hasnain M, Koneru JN, Gysel M and Baranchuk A: Clarithromycin, QTc interval prolongation and torsades de pointes: The need to study case reports. *Ther Adv Infect Dis* 1: 121-138, 2013.
53. Tisdale JE: Drug-induced QT interval prolongation and torsades de pointes: Role of the pharmacist in risk assessment, prevention and management. *Can Pharm J (Ott)* 149: 139-152, 2016.
54. Lo YC and Kuo CC: Temperature dependence of the biophysical mechanisms underlying the inhibition and enhancement effect of amiodarone on hERG channels. *Mol Pharmacol* 96: 330-344, 2019.
55. Shenthar J, Rachaiah JM, Pillai V, Chakali SS, Balasubramanian V and Chollenhalli Nanjappa M: Incidence of drug-induced torsades de pointes with intravenous amiodarone. *Indian Heart J* 69: 707-713, 2017.
56. Khan F, Ismail M, Khan Q and Ali Z: Moxifloxacin-induced QT interval prolongation and torsades de pointes: A narrative review. *Expert Opin Drug Saf* 17: 1029-1039, 2018.
57. Behzadi M, Joukar S and Beik A: Opioids and cardiac arrhythmia: A literature review. *Med Princ Pract* 27: 401-414, 2018.
58. Kasama M, Furukawa Y, Oguchi T, Hoyano Y and Chiba S: Effects of low temperature on the chronotropic and inotropic responses to zatebradine, E-4031 and verapamil in isolated perfused dog atria. *Jpn J Pharmacol* 78: 493-499, 1998.
59. Saeidnia S, Manayi A and Abdollahi M: From in vitro Experiments to in vivo and clinical studies: Pros and cons. *Curr Drug Discov Technol* 12: 218-224, 2015.
60. Zuppinger C, Gibbons G, Dutta-Passecker P, Segiser A, Most H and Suter TM: Characterization of cytoskeleton features and maturation status of cultured human iPSC-derived cardiomyocytes. *Eur J Histochem* 61: 2763, 2017.
61. Cai C, Wang S, Xu YJ, Zhang WL, Tang K, Ouyang Q, Lai LH and Pei JF: Transfer learning for drug discovery. *J Med Chem* 63: 8683-8694, 2020.

